

## CHAPTER 3

### EXACT AND APPROACH SOLUTION

#### 3.1 Exact Solution of One Dimensional Transient Conduction Problem

The nondimensionalized partial differential equation together with its boundary and initial conditions were solved analytically by the method of separation of variables here. The method of separation of variables was introduced by J. Fourier in 1820s and was based on expanding an arbitrary function in terms of Fourier series. The method has been applied by assuming the dependent variable to be a product of a number of functions, each being a function of a single independent variable. This reduces the partial differential equation to a system of ordinary differential equations, each being a function of a single independent variable.

In the case of transient conduction in a plane wall, for example, the dependent variable is the solution function which is expressed as  $\theta = X(\bar{x})\Gamma(\tau)$ , and the application of the method results in two ordinary differential equation, one in  $\bar{x}$  and the other in  $\tau$ .

The method is applicable if the geometry is simple and finite (such as a rectangular block, a cylinder or a sphere) so that the boundary surfaces has been described by simple mathematical functions, and the differential equation and the boundary and initial conditions in their most simplified form are linear and involve only one nonhomogeneous term. If the formulation involves a number of nonhomogeneous terms, the problem was split up into an equal number of simpler problems each involving only one homogeneous term, and then combining the solutions by superposition.

The analytical solutions of transient conduction problems typically involve infinite series, and thus the evaluation of an infinite number of terms to determine the temperature at a

specified location and time. If these infinite series were solved the exact solution can be defined as in Table 3.1 below.

**Table 3.1:** One dimensionless transient heat conduction exact solutions [12]

<b>Geometry</b>	<b>Solution</b>	<b><math>\lambda_n</math>' s are the roots of</b>
Plane wall	$\theta = \sum_{n=1}^{\infty} \frac{4 \sin \lambda_n}{2\lambda_n + \sin(2\lambda_n)} \cos(\lambda_n \bar{x}) e^{-\lambda^2 \tau}$	$Bi = \lambda_n \tan \lambda_n$
Cylinder	$\theta = \sum_{n=1}^{\infty} \frac{2}{\lambda_n} \frac{J_1(\lambda_n)}{J_0^2(\lambda_n) + J_1^2(\lambda_n)} J_0(\lambda_n \bar{r}) e^{-\lambda^2 \tau}$	$Bi = \lambda_n \frac{J_1(\lambda_n)}{J_0(\lambda_n)}$
Sphere	$\theta = \sum_{n=1}^{\infty} \frac{4(\sin \lambda_n - \lambda_n \cos \lambda_n)}{2\lambda_n - \sin(\lambda_n)} e^{-\lambda^2 \tau} \frac{\sin(\lambda_n \bar{r})}{(\lambda_n \bar{r})}$	$Bi = 1 - \lambda_n \cos \lambda_n$

## 3.2 Approximate and Graphical Solutions

### 3.2.1 One Term Approximation Solution

The analytical solution shown above for one dimensional transient heat conduction in a plane wall involves infinite series, which are difficult to evaluate. Therefore, it is suitable to simplify the analytical solutions and to present the solutions in tabular or graphical form using simple relations. The dimensionless quantities defined above for a plane wall also used for a cylinder or sphere by replacing the space variable  $x$  by  $r$  and the half thickness  $L$  by the outer radius  $r_0$ . It has been noted that the characteristic length in the definition of the Biot number is taken to be the half-thickness  $L$  for the plane wall, and the radius  $r_0$  for the long cylinder and sphere. The terms in the series in Table 3.1 converge rapidly with increasing time, and for  $\tau > 0.2$ , keeping the first term and neglecting all the remaining terms in the series results in an error under 2 percent. The solution has been usually used in the solution for times with  $\tau > 0.2$ , and thus it is very convenient to express the solution using this one term approximation, given as

$$\text{Plane wall} \quad \theta = A_1 \cos(\lambda_1 \bar{x}) e^{-\lambda_1^2 \tau} \quad \tau > 0.2 \quad (3.1)$$

$$\text{Cylinder} \quad \theta = A_1 J_0(\lambda_1 \bar{r}) e^{-\lambda_1^2 \tau} \quad \tau > 0.2 \quad (3.2)$$

$$\text{Sphere} \quad \theta = A_1 \frac{\sin(\lambda_1 \bar{r})}{(\lambda_1 \bar{r})} e^{-\lambda_1^2 \tau} \quad \tau > 0.2 \quad (3.3)$$

Where the constants  $A_1$  for three geometries are expressed as

$$A_1 = \frac{4 \sin \lambda_n}{2\lambda_n + \sin(2\lambda_n)} \quad \text{for plane wall} \quad (3.4)$$

$$A_1 = \frac{2}{\lambda_1} \frac{J_1(\lambda_1)}{J_0^2(\lambda_1) + J_1^2(\lambda_1)} \quad \text{for long cylinder} \quad (3.5)$$

$$A_1 = \frac{4(\sin \lambda_1 - \lambda_1 \cos \lambda_1)}{2\lambda_1 - \sin(\lambda_1)} \quad \text{for solid sphere} \quad (3.6)$$

The constants  $A_1$  and  $\lambda_1$  are functions of the Biot number only and their values are listed in Table 3.2. Once the Biot number is known, these relations can be used to determine the temperature anywhere in the medium. The determination of the constants  $A_1$  and  $\lambda_1$  usually requires interpolation. For those who prefer reading charts to interpolating, these relations are plotted and the one-term approximation solutions are presented in graphical

form, known as the transient temperature charts. It has been noted that the charts are sometimes difficult to read, and they are subject to reading errors. Therefore, the relations above should be preferred to the charts.

The transient temperature charts for a large plane wall, long cylinder and sphere has been presented by M. P. Heisler in 1947 and are called Heisler charts [1].

**Table 3.2:** Coefficients used in the one term approximate solution of transient one dimensional heat conduction [12]

Bi	Plane Wall		Long Cylinder		Solid Sphere	
	$\lambda_1$	$A_1$	$\lambda_1$	$A_1$	$\lambda_1$	$A_1$
0.1	0.3111	1.0161	0.4417	1.0246	0.5423	1.0298
0.2	0.4328	1.0311	0.6170	1.0483	0.7593	1.0592
0.3	0.5218	1.0450	0.7465	1.0712	0.9208	1.0880
0.4	0.5932	1.0580	0.8516	1.0931	1.0528	1.1164
0.5	0.6533	1.0701	0.9408	1.1143	1.1656	1.1441
0.6	0.7051	1.0814	1.0184	1.1345	1.2644	1.1713
0.7	0.7506	1.0918	1.0873	1.1539	1.3525	1.1978
0.8	0.7910	1.1016	1.1490	1.1724	1.4320	1.2236
0.9	0.8274	1.1107	1.2048	1.1902	1.5044	1.2488
1	0.8603	1.1191	1.2558	1.2071	1.5708	1.2732
2	1.0769	1.1785	1.5995	1.3384	2.0288	1.4793
3	1.1925	1.2102	1.7887	1.4191	2.2889	1.6227
4	1.2646	1.2287	1.9081	1.4698	2.4556	1.7202
5	1.3138	1.2403	1.9898	1.5029	2.5704	1.7870
6	1.3496	1.2479	2.0490	1.5253	2.6537	1.8338
7	1.3766	1.2532	2.0937	1.5411	2.7165	1.8673
8	1.3978	1.2570	2.1286	1.5526	2.7654	1.8920
9	1.4149	1.2598	2.1566	1.5611	2.8044	1.9106
10	1.4289	1.2620	2.1795	1.5677	2.8363	1.9249
20	1.4961	1.2699	2.2880	1.5919	2.9857	1.9781
30	1.5202	1.2717	2.3261	1.5973	3.0372	1.9898
40	1.5325	1.2723	2.3455	1.5993	3.0632	1.9942
50	1.5400	1.2727	2.3572	1.6002	3.0788	1.9962
100	1.5552	1.2731	2.3809	1.6015	3.1102	1.9990
$\infty$	1.5708	1.2732	2.4048	1.6021	3.1416	2.0000

### 3.2.2 Transient Dimensionless Temperature Charts

#### 3.2.2.1 Large Plane Wall Charts

Temperature time charts are useful for rapid estimation of temperature history in solids, and for some specific situations such charts can be prepared. Here it has been shown a plane wall of thickness  $2L$ , initially at a uniform temperature  $T_i$  and for times  $t > 0$  it is subjected to convection from both its surfaces into an ambient at a constant temperature  $T_\infty$  with a heat transfer coefficient  $h$ . Because of symmetry, the origin of the  $x$  coordinate at the centre of the plate has been chosen and only half of the plate has been considered.

In charts, there are the physical significance of the dimensionless parameters  $\tau$  and Biot number.

The dimensionless time  $\tau$  is shown in the form

$$\tau = \frac{\alpha t}{L^2} = \frac{k(1/L)L^2}{\rho c_p L^3 / t} \quad (3.7)$$

Thus, the Fourier number is a measure of the rate of heat conduction compared with the rate of heat storage in a given volume element. Therefore, the larger the Fourier number, the deeper the penetration of heat into a solid over a given time.

The physical significance of the Biot number that it is represented the ratio of the “internal thermal resistance” to the “external thermal resistance”.

The solution of the transient heat conduction problem is presented in the graphical form in Figure 3.1. Here Figure 3.1 gives the midplane temperature  $T_0$  or  $\theta_0$  at  $\bar{x} = 0$  as a function of the dimensionless time  $\tau$  for several different values of the parameter  $1/Bi$ . The curve for  $1/Bi=0$  corresponds to the case in which,  $h \rightarrow \infty$  or the surfaces of the plate are maintained at the ambient temperature  $T_\infty$  for large values of  $1/Bi$ , The Biot number is small, the internal conductance of the solid is large in comparison with the heat transfer coefficient at the surfaces. Figure 3.2 relates the temperature at six different locations within the slab to the midplane temperature  $T_0$ . Thus, given  $T_0$ , temperature at these locations can be determined. An examination of Figure 3.2 reveals that for values of  $1/Bi$  larger than 10 or  $Bi < 0.1$ , the temperature distribution within the slab may be considered

uniform with an error of less than about 2%; hence for such situation the spatial variation of temperature within the medium can be neglected.

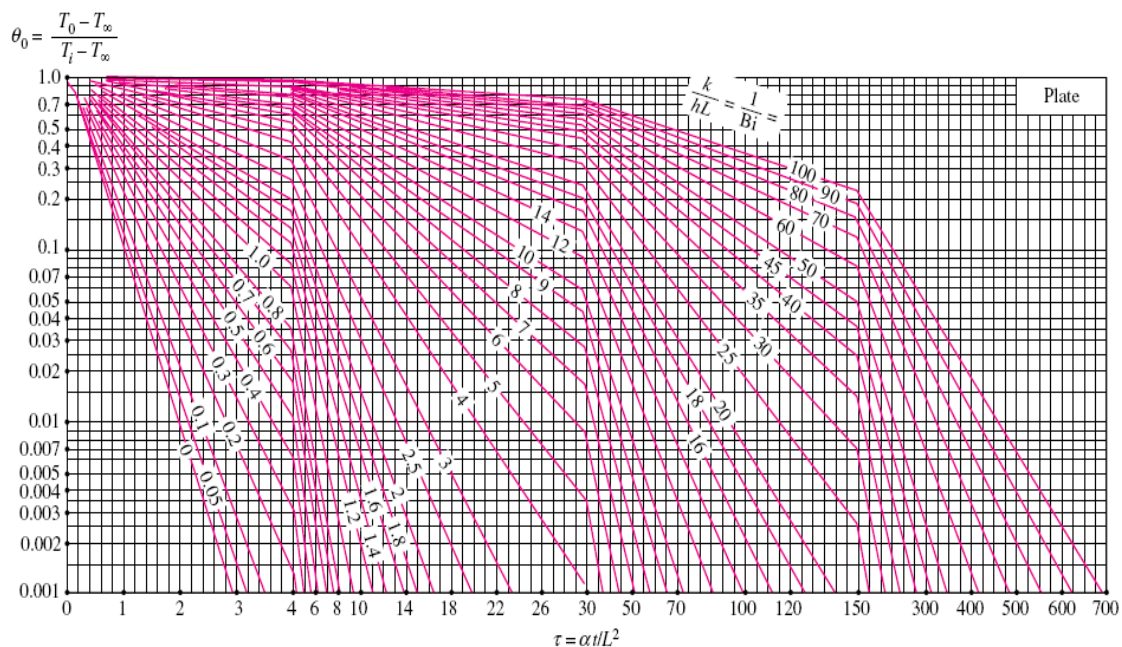


**Figure 3.1:** Midplane dimensionless temperature for plane wall

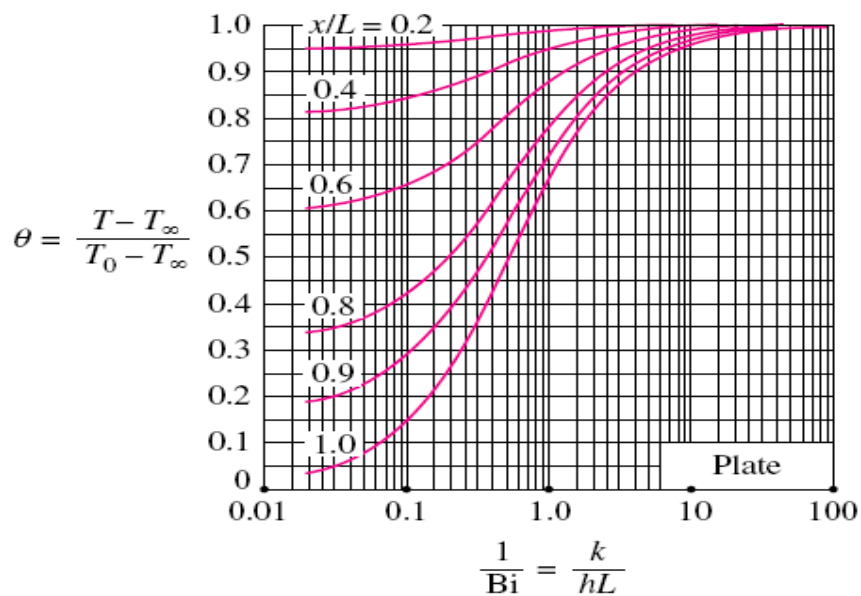


**Figure 3.2:** Dimensionless temperature distribution for plane wall

### 3.2.2.2 Long Cylinder Charts

In the previous section transient temperature charts presented for a slab of thickness  $2L$  subjected to convection at both surfaces. Now one dimensional, transient heat conduction in a long cylinder of radius  $r_0$ , which is initially at a uniform temperature  $T_i$  has been considered. Suddenly, at time  $t=0$ , the boundary surface at  $r = r_0$  is subjected to convection with a heat transfer coefficient  $h$  into an ambient at temperature  $T_\infty$  and maintained so for  $\tau > 0$ .

The solution of the transient heat conduction problem is presented in the graphical form for long cylinder in Figure 3.3. Here Figure 3.3 gives the midplane temperature  $\theta_0$  as a function of the dimensionless time  $\tau$  for several different values of the parameter  $1/Bi$ . The curve for  $1/Bi=0$  corresponds to the case in which,  $h \rightarrow \infty$ , or the surfaces of the cylinder are maintained at the ambient temperature  $T_\infty$ . Figure 3.4 relates the temperature at six different locations within the cylinder to the cylinder centreline temperature  $\theta_0$ . Thus, given  $\theta_0$ , temperature at these locations can be determined. An examination of Figure 3.4 reveals that for values of  $1/Bi$  larger than 10 or  $Bi < 0.1$ . The temperature distribution within the cylinder may be considered uniform with an error of less than about 2%; hence for such situation the spatial variation of temperature within the medium can be neglected.

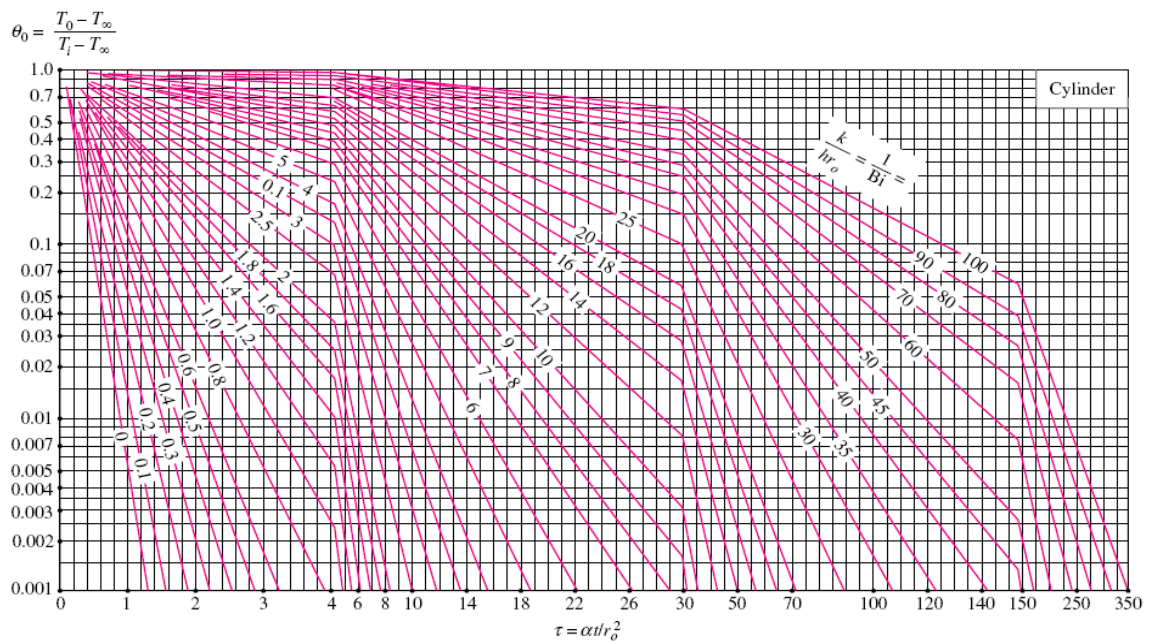


**Figure 3.3:** Centreline dimensionless temperature for long cylinder

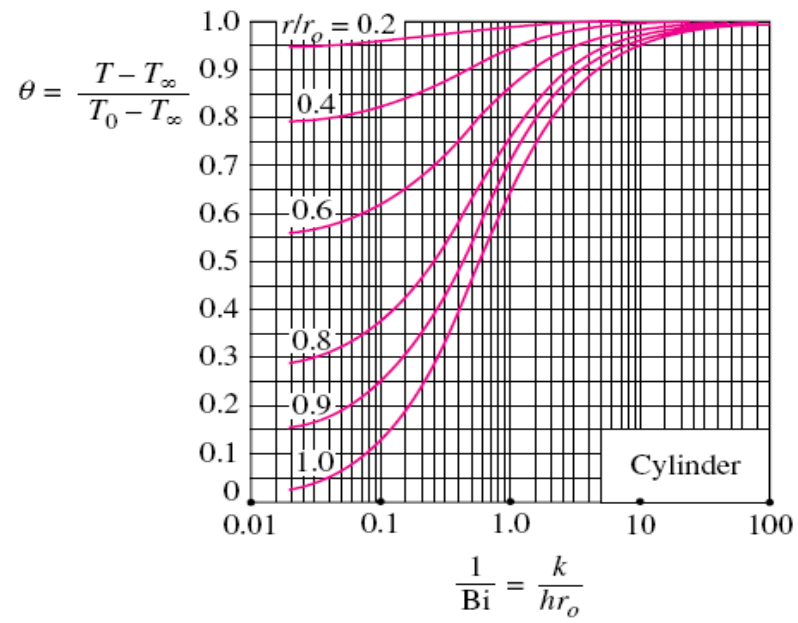


**Figure 3.4:** Dimensionless temperature distribution for long cylinder

### 3.2.2.3 Solid Sphere Charts

Transient temperature charts similar to those considered for long cylinder can also be constructed for the case of a solid sphere. Figure 3.5 gives the midplane temperature  $\theta_0$  as a function of the dimensionless time  $\tau$  for several different values of the parameter  $1/Bi$ . The curve for  $1/Bi=0$  corresponds to the case in which  $h \rightarrow \infty$  or the surfaces of the sphere are maintained at the ambient temperature  $T_\infty$ . Figure 3.6 relates the temperature at six different locations within the sphere centreline temperature  $\theta_0$ .

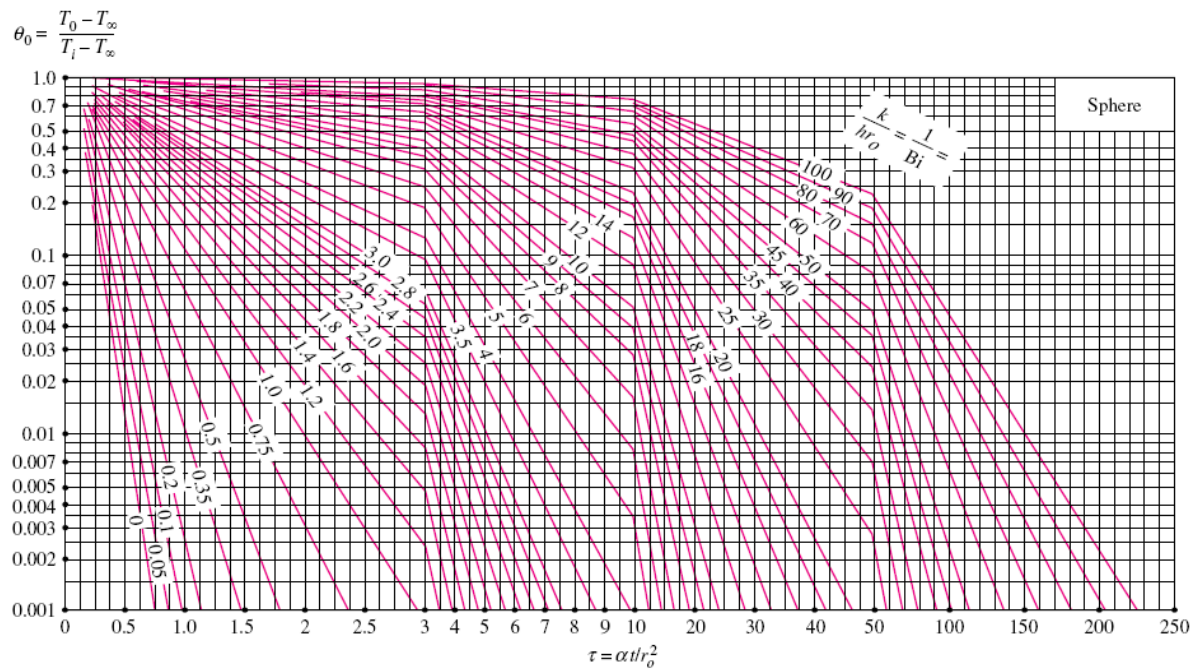


**Figure 3.5:** Midpoint dimensionless temperature for solid sphere

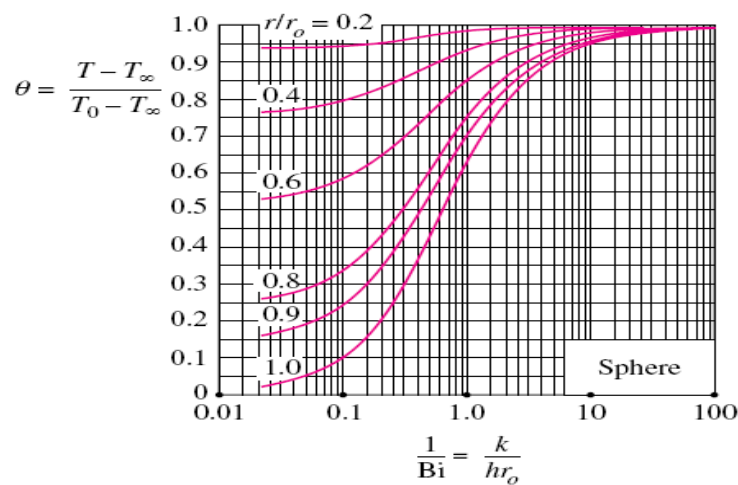


**Figure 3.6:** Dimensionless temperature distribution for solid sphere